

Asymptotic distribution of high-dimensional principal component scores connected to pervasive eigenvectors

Kristoffer Hellton, Magne Thoresen
Department of Biostatistics, University of Oslo,
P.O.Box 1122 Blindern N-0317, Oslo, Norway
k.h.hellton@medisin.uio.no

January 23, 2019

Abstract

Plots of scores from principal component analysis are a popular approach to visualize and explore high-dimensional genetic data. However, the inconsistency of the high-dimensional eigenvectors has discredited classical principal component analysis and helped motivate sparse principal component analysis where the eigenvectors are regularized. Still, classical principal component analysis is extensively and successfully used for data visualization, and our aim is to give an explanation of this paradoxical situation. We show that the visual information given by the relative positions of the scores will be consistent, if the related signal can be considered to be pervasive. Firstly, we argue that pervasive signals lead to eigenvalues scaling linearly with the dimension, and we discuss genetic applications where such pervasive signals are reasonable. Secondly, we prove within the high-dimension low sample size regime, that when eigenvalues scale linearly with the dimension, the sample component scores will appear as scaled and rotated versions of the population scores. In consequence, the relative positions and visual information conveyed by the score plots will be consistent.

Keywords: Genomics, High-dimensionality, Principal component analysis, Visualization.

1 Introduction

Principal component analysis is the workhorse of dimension reduction techniques in applied analyses, and works by building a small number of informative scores (Jolliffe, 2002). When analysing high-dimensional data with more variables than observations, these low-dimensional scores can be used directly for visualization or in conventional clustering and regression methods. The typical first step in analysis of high-dimensional genetic data is to visually explore plots of the principal component scores.

Principal component analysis reduces the data dimension by constructing orthogonal linear combinations of the variables, which express maximal variability. Let $\mathbf{X} = (\mathbf{x}_1, \dots, \mathbf{x}_n)$ be a $p \times n$ data matrix, where the observations $\mathbf{x}_i = (x_{i1}, \dots, x_{ip})^T$ are independent and identically distributed with $E(\mathbf{x}_i) = \mathbf{0}$ and $\text{var}(\mathbf{x}_i) = \Sigma$. With the eigenvalues and -vectors of Σ denoted by $\lambda_1 \geq \dots \geq \lambda_p$ and $\mathbf{v}_1, \dots, \mathbf{v}_p$, the population component scores and standardized population component scores are given as

$$\mathbf{s}_j^T = \mathbf{v}_j^T \mathbf{X}, \quad \mathbf{z}_j^T = \frac{\mathbf{v}_j^T \mathbf{X}}{\sqrt{\lambda_j}}, \quad (j = 1, \dots, p),$$

where we denote $\mathbf{z}_j = (z_{j1}, \dots, z_{jn})^T$ and $\mathbf{Z} = (\mathbf{z}_1, \dots, \mathbf{z}_p)^T$.

In applied data analysis, the principal components are based on the sample covariance matrix, $\hat{\Sigma} = \frac{1}{n-1} \sum_{i=1}^n (\mathbf{x}_i - \bar{\mathbf{x}})(\mathbf{x}_i - \bar{\mathbf{x}})^T$, and the sample eigenvalues and -vectors, $d_1 \geq \dots \geq d_p$ and $\hat{\mathbf{v}}_1, \dots, \hat{\mathbf{v}}_p$. The sample component scores and standardized sample component scores are then denoted as

$$\hat{\mathbf{s}}_j^T = \hat{\mathbf{v}}_j^T \mathbf{X}, \quad \hat{\mathbf{z}}_j^T = \frac{\hat{\mathbf{v}}_j^T \mathbf{X}}{\sqrt{d_j}}, \quad (j = 1, \dots, p).$$

We consider the spiked covariance model (Johnstone, 2001), where the m first population eigenvalues are substantially larger than the remaining eigenvalues.

The asymptotic consistency of principal component analysis has attracted substantial attention the last decade, and it has been shown that, while principal component analysis is consistent when p is fixed and $n \rightarrow \infty$ (Anderson, 1963), the sample eigenvectors and -values are generally inconsistent in the high-dimensional case. Paul (2007) and Johnstone & Lu (2009) proved this for fixed population eigenvalues when $p, n \rightarrow \infty$ at a constant ratio, $p/n = \gamma > 0$. Jung & Marron (2009) introduced the high-dimension low sample size

asymptotic framework, where the sample size is fixed and the m first eigenvalues grow with the dimension p as

$$\lambda_j = \sigma_j^2 p^\alpha, \quad (j = 1, \dots, m).$$

Here the consistency of principal component analysis depends on α as $p \rightarrow \infty$. The sample eigenvectors are consistent when $\alpha > 1$, while they are strongly inconsistent when $\alpha < 1$. Jung et al. (2012) proved that for $\alpha = 1$, the consistency is described by a limiting distribution depending on n .

As a consequence of the eigenvector inconsistency, Johnstone & Lu (2009) argued that the principal components should have a sparse representation, further motivating the development of sparse principal component analysis and the regularization of eigenvectors (Zou et al., 2006; Witten et al., 2009). Cai & Zhou (2012) states: “It is now well understood that in the high-dimensional setting the standard sample covariance matrix does not provide satisfactory performance and regularization is needed.”

However, in many genomic applications, the use of principal component analysis and score plots continued with great success, suggesting that the scores are suitable for analysis in some situations. As Lee et al. (2010) noted: “Inconsistency of the sample eigenvectors does not necessarily imply poor performance of principal component analysis”. We explore this paradoxical situation and try to bridge the gap between the theoretical inconsistency and the practical usefulness. Parts of the explanation was given by Shen et al. (2012), showing that, when $\alpha > 1$ in high-dimension low sample size framework, the sample scores are scaled versions of the population scores, and by Yang et al. (2014), proving that principal component scores will correctly identify strata in a stratified population.

In this paper, we focus on the concept of pervasive effects and demonstrate how these can lead to population eigenvalues scaling linearly with the dimension. Under this eigenvalue assumption, we derive the joint asymptotic distribution of the sample principal component scores and explore the impact on the visual information conveyed by score plots. A key point is the interpretation of the eigenvalue assumption as a consequence of the data structure. In our opinion, it is easier to relate to an assumption regarding the data-generating mechanism than an assumption about the eigenvalues.

2 Pervasiveness and eigenvalues

In this section, we demonstrate how an assumption regarding the data-generating mechanism, specifically pervasive eigenvector coefficients, can lead to eigenvalues scaling linearly with the dimension, or the case of $\alpha = 1$ in the high-dimension low sample size regime. In the econometrics literature, the concept of pervasiveness is commonly used for latent factor estimation (Fan et al., 2013; Bai & Liao, 2012). A pervasive factor is here thought to be an unobserved variable affecting a substantial proportion of the observed variables. In a situation where the dimension increases, pervasiveness can be formulated in terms of the asymptotic proportion of non-zero variable coefficients:

Definition 1. *A sequence of p -dimensional vectors $\mathbf{v} = (v_1, \dots, v_p)^T$ fulfils the pervasiveness assumption, if the proportion of non-zero entries $r_p = \frac{1}{p} \sum_{i=1}^p I_{\{v_i^2 > 0\}}$ fulfils:*

$$\lim_{p \rightarrow \infty} r_p > 0.$$

For the spiked covariance model (Johnstone, 2001; Nadler, 2008; Johnstone & Lu, 2009) with a single component, each observation is given by

$$\mathbf{x}_i = \mathbf{v}z_i + \varepsilon_i, \quad \text{var}(\varepsilon_i) = \sigma^2 I, \quad \text{var}(z_i) = 1, \quad (i = 1, \dots, n), \quad (1)$$

and the covariance matrix of \mathbf{x}_i will be $\Sigma = \mathbf{v}\mathbf{v}^T + \sigma^2 I$. The normalized vector $\mathbf{v}/\|\mathbf{v}\|$ is an eigenvector of $\mathbf{v}\mathbf{v}^T$ and therefore also an eigenvector of Σ . The corresponding eigenvalue of $\mathbf{v}\mathbf{v}^T$ is given by $\|\mathbf{v}\|^2 = \sum_{j=1}^p v_j^2$. Thus, the largest eigenvalue of Σ is $\lambda_1 = \sum_{j=1}^p v_j^2 + \sigma^2$ and the dependence on the dimension p is given by the coefficients of \mathbf{v} .

If the values of v_1, \dots, v_p are constant and fulfils the pervasiveness assumption, there exist two constants $c_1 \leq r_p \min_j v_j^2$ and $c_2 \geq r_p \max_j v_j^2$, such that λ_1 is bounded by

$$c_1 p + \sigma^2 \leq \lambda_1 \leq c_2 p + \sigma^2.$$

The first eigenvalue will therefore scale linearly with the dimension as $p \rightarrow \infty$, while the other eigenvalues will remain constant. This argument also extends to m components.

One can also interpret pervasive signals in terms of the covariance matrix $\Sigma = \mathbf{v}\mathbf{v}^T + \sigma^2 I$ with the off-diagonal elements $\Sigma_{jk} = v_j v_k$. Based on the coefficients of \mathbf{v} , we can group the non-zero elements of the covariance matrix into blocks. We illustrate this situation by

a covariance matrix consisting of three separate independent blocks, where all variables within each block are equally correlated. Each block will then have an eigenvector with equal, non-zero coefficients for the variables within the block and zeros for the others. If the dimension of each block remains a proportion of the total number of variables as $p \rightarrow \infty$, the corresponding eigenvectors will be pervasive.

Assume Σ to be divided into different independent sub-matrices:

$$\Sigma = \begin{bmatrix} \Sigma_1 & 0 & \dots & 0 \\ 0 & \Sigma_2 & 0 & \vdots \\ \vdots & 0 & \Sigma_3 & 0 \\ 0 & \dots & 0 & \sigma^2 I \end{bmatrix}, \quad \Sigma_j = \sigma^2 \begin{bmatrix} 1 & \rho_j & \dots & \rho_j \\ \rho_j & 1 & & \\ \vdots & & \ddots & \rho_j \\ \rho_j & & \rho_j & 1 \end{bmatrix}, \quad (j = 1, 2, 3).$$

with $1 > \rho_1 > \rho_2 > \rho_3 > 0$. If the dimension of Σ_j is given by $r_j p$, where r_j is a non-zero proportion, $1 \geq r_1 + r_2 + r_3 > 0$, the covariance matrix Σ will have three spiked eigenvalues

$$\lambda_1 = \sigma^2 (\rho_1 r_1 p + 1 - \rho_1), \quad \lambda_2 = \sigma^2 (\rho_2 r_2 p + 1 - \rho_2), \quad \lambda_3 = \sigma^2 (\rho_3 r_3 p + 1 - \rho_3),$$

scaling linearly with the dimension, while the remaining $p - 3$ eigenvalues are constant. Each of the spiked eigenvalues represents one block of variables and the importance of the block is determined by the proportion r_j and the degree of correlation within the cluster ρ_j . A pervasive eigenvector can therefore also be interpreted as a block of variables, where the dimension is a non-vanishing proportion of the total number of variables.

2.1 Single nucleotide polymorphisms (SNPs)

An example of a pervasive association is the relationship between ethnicity and genomic markers, known as SNPs. These are genetic loci with at least two alleles with an allelic frequency in a population. The neutral theory of molecular evolution states that allele frequencies at most genetic loci change due to two stochastic processes; mutation and random drift. When comparing SNPs from various ethnic populations, the random allelic drift is the main driver of variation and the markers that differ between ethnicities will be many and randomly distributed. If new SNP markers are included in the analysis, we expect a certain proportion to be informative with respect to ethnicity, and this corresponds the notion of pervasive associations. SNP markers are commonly used to correct for confounding by ethnicity (Price et al., 2006; Patterson et al., 2006).

Based on the premiss that ethnicity has a pervasive effect on SNP markers, we can assume that the corresponding eigenvalue scales linearly with the number of included variables. Also, due to the random drift, two populations will diverge over time and accumulate a larger proportion of differentiating markers. We can therefore expect larger eigenvalues when comparing European and Japanese populations, than when comparing e.g. northern and southern Japanese populations.

3 Asymptotic distribution of sample scores

This section presents the asymptotic distribution of the sample principal component scores in the high-dimension low sample size framework, under the same general conditions (C_1) and (C_2) as specified by Jung et al. (2012):

- (C1) The standardized principal component scores have finite fourth moments $E(\mathbf{z}_i)^4 < \infty$, and are uncorrelated, but possibly dependent, fulfilling the ρ -mixing condition.

The ρ -mixing condition is satisfied if the maximal correlation coefficient defined as

$$\rho(m) = \sup_{j,f,g} |\text{cor}(f,g)|, \quad f \in L_2(\mathcal{F}_{-\infty}^j), g \in L_2(\mathcal{F}_{j+m}^\infty),$$

where \mathcal{F}_K^L is the σ -field of events generated by the variables $\mathbf{z}_i, K \leq i \leq L$, will approach zero, $\rho(m) \rightarrow 0$, as $m \rightarrow \infty$.

- (C2) The non-spiked eigenvalues $\lambda_{m+1}, \dots, \lambda_p$ fulfill

$$\frac{\sum_{i=m+1}^p \lambda_i^2}{\left(\sum_{i=m+1}^p \lambda_i\right)^2} \rightarrow 0, \quad \frac{1}{p} \sum_{i=m+1}^p \lambda_i \rightarrow \tau^2, \quad p \rightarrow \infty.$$

Let the $n \times p$ matrix \mathbf{Z} be the the population standardized principal component scores. For an m spiked model, the following notation for the scaled population scores is introduced:

$$\tilde{\mathbf{Z}}_{1:m} = (\sigma_1 \mathbf{z}_1, \dots, \sigma_m \mathbf{z}_m),$$

which gives the $m \times m$ matrix $\mathbf{W} = \tilde{\mathbf{Z}}_{1:m}^T \tilde{\mathbf{Z}}_{1:m}$. The stochastic eigenvalues of the matrix are denoted by $d_j(\mathbf{W})$ and the stochastic eigenvectors are denoted by $\mathbf{v}_j(\mathbf{W})$ for $j = 1, \dots, p$.

Theorem 1. Under conditions (C_1) , (C_2) and assuming the m spiked eigenvalues to scale linearly with the dimension,

$$\lambda_1 = \sigma_1^2 p, \quad \lambda_2 = \sigma_2^2 p \quad \cdots \quad \lambda_m = \sigma_m^2 p,$$

the sample principal component scores converge to the following limiting distribution jointly for $j = 1, \dots, m$:

$$\hat{z}_{ij} \rightarrow \sqrt{\frac{n}{d_j(\mathbf{W})}} (\sigma_1 z_{i1}, \dots, \sigma_m z_{im}) \mathbf{v}_j(\mathbf{W}) = \sqrt{\frac{n}{d_j(\mathbf{W})}} \sum_{l=1}^m \sigma_l z_{il} v_{jl}(\mathbf{W}), \quad (2)$$

where $d_j(\mathbf{W})$ and $\mathbf{v}_j(\mathbf{W})$ are the j th eigenvalues and eigenvectors of the stochastic matrix \mathbf{W} . The joint distribution of sample principal component scores are given in matrix notation as

$$\begin{bmatrix} \hat{z}_{i1} \\ \vdots \\ \hat{z}_{im} \end{bmatrix} \xrightarrow{d} \begin{bmatrix} \sqrt{n/d_1(\mathbf{W})} & & 0 \\ & \ddots & \\ 0 & & \sqrt{n/d_m(\mathbf{W})} \end{bmatrix} \begin{bmatrix} \mathbf{v}_1(\mathbf{W}) & \cdots & \mathbf{v}_m(\mathbf{W}) \end{bmatrix} \begin{bmatrix} \sigma_1 z_{i1} \\ \vdots \\ \sigma_m z_{im} \end{bmatrix}, \quad (i = 1, \dots, n).$$

The proof of Theorem 1 is based on Lemma 1 and 2.

Lemma 1 (Jung et al. (2012)). Under Conditions $(C1)$ and $(C2)$ and the assumption of linearly increasing eigenvalues

$$\lambda_1 = \sigma_1^2 p, \quad \lambda_2 = \sigma_2^2 p \quad \cdots \quad \lambda_m = \sigma_m^2 p,$$

the sample eigenvalues converge in distribution

$$p^{-1} d_j \xrightarrow{d} \begin{cases} d_j(\mathbf{W})/n + \tau^2/n, & (j = 1, \dots, m), \\ \tau^2/n, & (j = m + 1, \dots, p), \end{cases}$$

and the sample eigenvectors are given by

$$\hat{\mathbf{v}}_j^T \mathbf{v}_k = \sqrt{\frac{\lambda_k}{n d_j}} \mathbf{z}_k^T \hat{\mathbf{u}}_j, \quad (j = 1, \dots, m; k = 1, \dots, p), \quad (3)$$

where $\hat{\mathbf{u}}_j$, the j th sample eigenvector of $p^{-1} \mathbf{X}^T \mathbf{X} = p^{-1} \sum_{k=1}^p \lambda_k \mathbf{z}_k \mathbf{z}_k^T$, converges in distribution to

$$\hat{\mathbf{u}}_j \xrightarrow{d} \frac{\tilde{\mathbf{Z}}_{1:m} \mathbf{v}_j(\mathbf{W})}{\sqrt{d_j(\mathbf{W})}}, \quad p \rightarrow \infty.$$

Lemma 2 (Jung et al. (2012)). *Under Conditions (C1) and (C2), the standardized population scores for the non-spiked eigenvalues converge in probability to*

$$\frac{1}{p} \sum_{i=m+1}^p \lambda_i \mathbf{z}_i \mathbf{z}_i^T \xrightarrow{P} \tau^2 I_n.$$

of Theorem 1. The standardized sample principal component scores can be decomposed into the spiked and non-spiked eigenvalues, and expression (3) and the spiked population eigenvalues give

$$\begin{aligned} \hat{z}_{ij} &= d_j^{-1/2} \sum_{k=1}^p \lambda_k^{1/2} z_{ik} \hat{\mathbf{v}}_j^T \mathbf{v}_k = \frac{1}{\sqrt{nd_j}} \left(\sum_{k=1}^m \lambda_k z_{ik} \mathbf{z}_k^T + \sum_{k=m+1}^p \lambda_k z_{ik} \mathbf{z}_k^T \right) \hat{\mathbf{u}}_j \\ &= \frac{1}{\sqrt{np^{-1}d_j}} \left(\sum_{k=1}^m \sigma_k^2 z_{ik} \mathbf{z}_k^T + \frac{1}{p} \sum_{k=m+1}^p \lambda_k z_{ik} \mathbf{z}_k^T \right) \hat{\mathbf{u}}_j, \quad (i = 1, \dots, n; j = 1, \dots, m). \end{aligned}$$

When $p \rightarrow \infty$, the sample eigenvalues, d_j , converge according to Lemma 1, while the term consisting of the non-spiked eigenvalues can be rewritten as the vector

$$\frac{1}{p} \sum_{k=m+1}^p \lambda_k z_{ik} \mathbf{z}_k^T = \left[\frac{1}{p} \sum_{k=m+1}^p \lambda_k z_{ik} z_{1k}, \dots, \frac{1}{p} \sum_{k=m+1}^p \lambda_k z_{ik}^2, \dots, \frac{1}{p} \sum_{k=m+1}^p \lambda_k z_{ik} z_{nk} \right]^T. \quad (4)$$

By Lemma 2, a version of the law of large numbers, the entries of the vector converges for fixed m to $\frac{1}{p} \sum_{k=m+1}^p \lambda_k z_{ik} z_{lk} \rightarrow 0$ for $l \neq i$, while the i th entry converges to $\frac{1}{p} \sum_{k=m+1}^p \lambda_k z_{ik}^2 \rightarrow \tau^2$. The vector in (4) will converge to a unit vector, $\mathbf{e}_i = (0, 0, \dots, 0, 1, 0, \dots, 0)^T$ with only a non-zero entry at position i scaled by τ^2 :

$$\frac{1}{p} \sum_{k=m+1}^p \lambda_k z_{ik} \mathbf{z}_k^T \rightarrow \tau^2 \mathbf{e}_i^T.$$

The standardized sample principal component score will then converge in distribution to

$$\begin{aligned} \hat{z}_{ij} &\xrightarrow{d} \frac{\sqrt{n}}{(d_j(\mathbf{W}) + \tau^2)} \left(\sum_{k=1}^m \sigma_k^2 z_{ik} \mathbf{z}_k^T + \tau^2 \mathbf{e}_i^T \right) \frac{\tilde{\mathbf{Z}}_{1:m} \mathbf{v}_j(\mathbf{W})}{\sqrt{d_j(\mathbf{W})}} \\ &= \frac{\sqrt{n}}{(d_j(\mathbf{W}) + \tau^2) \sqrt{d_j(\mathbf{W})}} \left(\sum_{k=1}^m z_{ik} \sigma_k^2 \mathbf{z}_k^T \tilde{\mathbf{Z}}_{1:m} \mathbf{v}_j(\mathbf{W}) + \tau^2 \mathbf{e}_i^T \tilde{\mathbf{Z}}_{1:m} \mathbf{v}_j(\mathbf{W}) \right). \quad (5) \end{aligned}$$

The expression in the first term corresponds to the k th row of \mathbf{W} and with the eigenequation $\mathbf{W} \mathbf{v}_j(\mathbf{W}) = d_j(\mathbf{W}) \mathbf{v}_j(\mathbf{W})$, the term can be rewritten as

$$\sigma_k \mathbf{z}_k^T \tilde{\mathbf{Z}}_{1:m} \mathbf{v}_j(\mathbf{W}) = d_j(\mathbf{W}) v_{jk}(\mathbf{W}),$$

while the unit vector in the second term gives

$$\mathbf{e}_i^T \tilde{\mathbf{Z}}_{1:m} \mathbf{v}_j(\mathbf{W}) = [\sigma_1 z_{i1}, \dots, \sigma_m z_{im}] \mathbf{v}_j(\mathbf{W}) = \sum_{k=1}^m \sigma_k z_{ik} v_{jk}(\mathbf{W}).$$

Expression (5) can then be simplified to

$$\hat{z}_{ij} \xrightarrow{d} \frac{\sqrt{n} (d_j(\mathbf{W}) + \tau^2)}{(d_j(\mathbf{W}) + \tau^2) \sqrt{d_j(\mathbf{W})}} \sum_{k=1}^m \sigma_k z_{ik} v_{jk}(\mathbf{W}) = \sqrt{\frac{n}{d_j(\mathbf{W})}} \sum_{k=1}^m \sigma_k z_{ik} v_{jk}(\mathbf{W}).$$

□

The first matrix, given by the sample eigenvalues, is a diagonal matrix and will act as a *scaling matrix*. The second matrix, given by the m sample eigenvectors, is an orthogonal matrix and will therefore act as an m -dimensional *rotation matrix*. Thus, the m -dimensional sample score vector will be a scaled and rotated version of the population score vector in m -dimensional space.

4 Implications for visualizations

When principal component scores are used to visualize high-dimensional data, it is common to display the m first important sample scores in two-dimensional plots (or possibly in 3D). These score plots can be used to compare observations, detect subgroups or identify outliers. Theorem 1 shows that plots of the sample scores can still give valid information about the population scores, despite the inconsistent eigenvectors. First, we present the special cases of $m = 1$ and $m = 2$, and then the general result for $m > 2$.

For a single component, \mathbf{W} will be a scalar such that sample eigenvalue is $d_1(\mathbf{W}) = \sigma_1^2 \mathbf{z}_1^T \mathbf{z}_1$ and the eigenvector is simply 1. The first sample principal component score will therefore converge in distribution to a scaled version of the population score

$$\hat{z}_{i1} \rightarrow \sigma_1 \sqrt{\frac{n}{d_1(\mathbf{W})}} z_{i1}, \quad (i = 1, \dots, n).$$

If the population scores are independently and identically normally distributed, $z_{ij} \sim \mathcal{N}(0, 1)$, the first eigenvalue is distributed as $d_1(\mathbf{W}) \sim \sigma_1^2 \chi_n^2$, a scaled chi-squared distribution with n degrees of freedom. This is the same distribution found by Shen et al. (2012) in the $\alpha > 1$ -case.

For $m = 2$, the sample scores converge in distribution to

$$\begin{bmatrix} \hat{z}_{i1} \\ \hat{z}_{i2} \end{bmatrix} \rightarrow \underbrace{\begin{bmatrix} \sqrt{\frac{n}{d_1(\mathbf{W})}} & 0 \\ 0 & \sqrt{\frac{n}{d_2(\mathbf{W})}} \end{bmatrix}}_{\text{Scaling}} \underbrace{\begin{bmatrix} v_{11}(\mathbf{W}) & v_{12}(\mathbf{W}) \\ v_{12}(\mathbf{W}) & v_{22}(\mathbf{W}) \end{bmatrix}}_{\text{Rotation}} \begin{bmatrix} \sigma_1 z_{i1} \\ \sigma_2 z_{i2} \end{bmatrix}, \quad (i = 1, \dots, n).$$

The sample score vector is a scaled and rotated version of the population score vector. When there are more than two important components, one typically selects pairs of scores and plot these against each other. The distribution of a pair of the j th and k th sample principal component scores can for $m > 2$ be decomposed into two parts:

$$\begin{bmatrix} \hat{z}_{ij} \\ \hat{z}_{ik} \end{bmatrix} \xrightarrow{d} \underbrace{\begin{bmatrix} \sqrt{\frac{n}{d_j(\mathbf{W})}} & 0 \\ 0 & \sqrt{\frac{n}{d_k(\mathbf{W})}} \end{bmatrix}}_{\text{Scaling}} \underbrace{\begin{bmatrix} v_{jj}(\mathbf{W}) & v_{kj}(\mathbf{W}) \\ v_{jk}(\mathbf{W}) & v_{kk}(\mathbf{W}) \end{bmatrix}}_{\text{Approximate rotation}} \begin{bmatrix} \sigma_j z_{ij} \\ \sigma_k z_{ik} \end{bmatrix} + \underbrace{\begin{bmatrix} \varepsilon_{ij} \\ \varepsilon_{ik} \end{bmatrix}}_{\text{Noise}}, \quad (6)$$

for $i = 1, \dots, n$, where

$$\varepsilon_{ij} = \sqrt{\frac{n}{d_j(\mathbf{W})}} \sum_{l=1, l \neq j, k}^m \sigma_l z_{il} v_{jl}(\mathbf{W}), \quad \varepsilon_{ik} = \sqrt{\frac{n}{d_k(\mathbf{W})}} \sum_{l=1, l \neq j, k}^m \sigma_l z_{il} v_{kl}(\mathbf{W}).$$

In the case of normally distributed scores, we can use simulations and large n asymptotics to evaluate the distribution of the last term in Eq. (6). It is seen that in practice, these terms can be considered as noise compared to the scaling and approximate rotation. This assertion depends, however, on the size of the sample, n , relative to the signal strengths $\sigma_1^2, \dots, \sigma_m^2$. This is illustrated in a practical data example in the Appendix. When $z_{ij} \sim \mathcal{N}(0, 1)$, the matrix \mathbf{W} will be Wishart distributed and, in case of large n , the distributions of $d_j(\mathbf{W})$ and $v_{jl}(\mathbf{W})$ are known. In the Appendix, these distributions are used to establish the asymptotic variance of ε_{ij} :

$$\text{var}(\varepsilon_{ij}) = \frac{1}{n} \sum_{l=1, l \neq j, k}^m \left(\frac{\sigma_j^2}{\sigma_l^2} - 1 \right)^{-2} + O(n^{-1}), \quad (7)$$

Based on Eq. (7) one can see that the largest ratio between the signal strengths of the component pair in question and the signal strengths of all the other components, $\sigma_j^2/\sigma_l^2, l \neq$

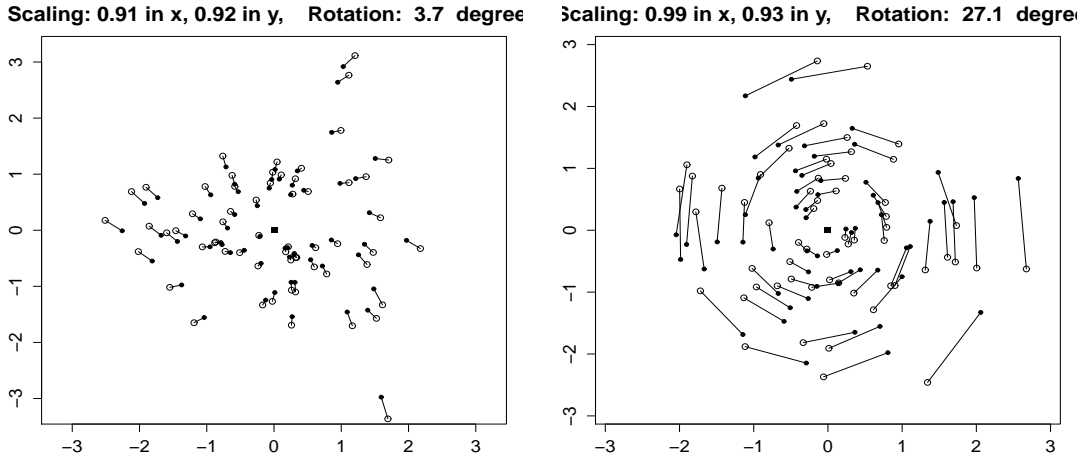


Figure 1: Difference in sample (black dots) and population (circles) principal component scores displaying a) scaling, b) rotation.

j, k , will be the main driver behind the noise variation. The consequence is that the noise can become large if one of the components in the pair has one or more neighbouring components with similar signal strength σ_l^2 .

When the noise part is negligible, the joint distribution in (6) shows that a two-dimensional plot of the estimated j th and k th sample principal component scores will be a scaled and approximately rotated version of the two-dimensional plot of the population principal component scores. Thus the relative positions of the population scores, and thereby the visual information, will be preserved by the sample scores. The behaviour of the scaling matrix and the approximate rotation matrix will depend on the distribution of the random eigenvalues and -vectors, $d_j(\mathbf{W})$ and $\mathbf{v}_j(\mathbf{W})$. According to the different outcomes of these quantities, the visualization of the sample scores compared to the population scores will behave quite differently. We can divide this behaviour into three main cases: mainly scaling, mainly rotation or a so-called saddle point.

Firstly, if the scaling of both components is either significantly smaller or larger than 1, but there is no significant rotation, the sample scores will appear as a radial shift outwards or inwards from the origin, compared to the population scores. This is seen in Figure 1a). This situation would be more common if the difference between the two signal strengths

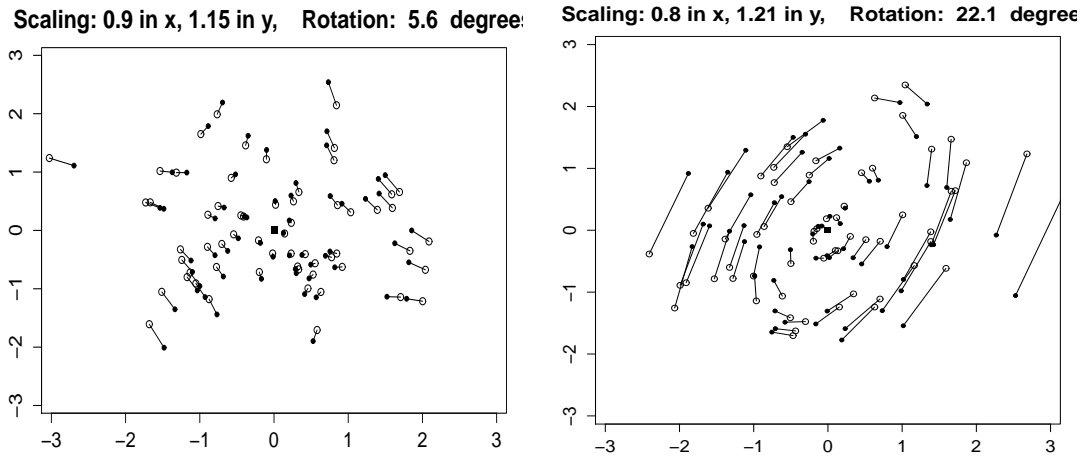


Figure 2: Difference in sample (black dots) and population (circles) principal component scores displaying a a) saddle point, b) fault.

are large, such that the corresponding eigenvalues are well-separated. Secondly, if the approximate rotation is large, but the scaling in each direction is insignificant, the sample scores will appear as a rotation of the population scores around the origin in positive or negative angular direction, as seen in Figure 1b). This situation would be more common if the two signal strengths are similar, such that the corresponding eigenvalues are not well-separated. Then, the estimated eigenvectors are only able to estimate the two-dimensional subspace spanned by the eigenvectors, and not the individual eigenvectors.

Lastly, we can have the special case seen in Figure 2a), where the scaling is significant, but smaller than 1 in one direction and larger than 1 in the other direction. An equivalent to this situation is found in the theory of linear dynamical systems, where it is termed a saddle point (Jordan & Smith, 2007, p. 66). If we in addition have a large rotation, one will instead see a fault-like rotation, as seen in Figure 2b).

5 Conclusion

The use of classical principal component analysis in the high-dimensional setting suffers from a paradoxical situation: the eigenvectors and scores are not asymptotically consistent,

but in practice the method is highly successful. This gap can hopefully be bridged by highlighting how the visualization of the population structures will perform for pervasive signals. It has been shown that for principal components with eigenvalues scaling linearly with the dimension, the relative positions and visual information of pairs of principal component scores will be consistent for practical purposes. Further, we argue that if a signal can be considered pervasive, such as different ethnicity effects genomic SNP markers, the connected eigenvalues will scale linearly with the dimension and the asymptotic results can be thought to be valid.

Acknowledgements

The authors would like to thank J. S. Marron for discussions and encouragements. The work was supported by the Norwegian Cancer Society.

References

- ANDERSON, T. (1963). Asymptotic theory for principal component analysis. *Ann. Statist.* **34**, 122–148.
- BAI, J. & LIAO, Y. (2012). Efficient estimation of approximate factor models via regularized maximum likelihood. *arXiv preprint arXiv:1209.5911* .
- CAI, T. T. & ZHOU, H. H. (2012). Minimax estimation of large covariance matrices under l_1 norm. *Statist. Sinica* **22**, 1319–1349.
- FAN, J., LIAO, Y. & MINCHEVA, M. (2013). Large covariance estimation by thresholding principal orthogonal complements. *J. R. Statist. Soc. B* **75**, 603–680.
- JOHNSTONE, I. M. (2001). On the distribution of the largest eigenvalue in principal components analysis. *Ann. Statist.* **29**, 295–327.
- JOHNSTONE, I. M. & LU, A. Y. (2009). On consistency and sparsity for principal components analysis in high dimensions. *JASA* **104**, 682–693.
- JOLLIFFE, I. T. (2002). *Principal component analysis*. New York: Springer.

- JORDAN, D. W. & SMITH, P. (2007). *Nonlinear ordinary differential equations: an introduction for scientists and engineers*. New York.
- JUNG, S. & MARRON, J. S. (2009). PCA consistency in high dimension, low sample size context. *Ann. Statist.* **37**, 4104–4130.
- JUNG, S., SEN, A. & MARRON, J. S. (2012). Boundary behavior in high dimension, low sample size asymptotics of PCA. *J. Mult. Anal.* **109**, 190–203.
- LEE, S., ZOU, F. & WRIGHT, F. A. (2010). Convergence and prediction of principal component scores in high-dimensional settings. *Ann. Statist.* **38**, 3605.
- MUIRHEAD, R. J. (2009). *Aspects of multivariate statistical theory*, vol. 197. Wiley. com.
- NADLER, B. (2008). Finite sample approximation results for principal component analysis: A matrix perturbation approach. *Ann. Statist.* **36**, 2791–2817.
- PATTERSON, N., PRICE, A. L. & REICH, D. (2006). Population structure and eigenanalysis. *PLoS Genetics* **2**, e190.
- PAUL, D. (2007). Asymptotics of sample eigenstructure for a large dimensional spiked covariance model. *Stat. Sinica* **17**, 1617–1642.
- PEROU, C. M., SØRLIE, T., EISEN, M. B., VAN DE RIJN, M., JEFFREY, S. S., REES, C. A., POLLACK, J. R., ROSS, D. T., JOHNSEN, H., AKSLEN, L. A. et al. (2000). Molecular portraits of human breast tumours. *Nature* **406**, 747–752.
- PRICE, A. L., PATTERSON, N. J., PLENGE, R. M., WEINBLATT, M. E., SHADICK, N. A. & REICH, D. (2006). PCA corrects for stratification in genome-wide association studies. *Nature Genet.* **38**, 904–909.
- SHEN, D., SHEN, H., ZHU, H. & MARRON, J. S. (2012). High dimensional principal component scores and data visualization. *arXiv preprint arXiv:1211.2679* .
- WITTEN, D. M., TIBSHIRANI, R. & HASTIE, T. (2009). A penalized matrix decomposition, with applications to sparse principal components and canonical correlation analysis. *Biostatistics* **10**, 515–534.

YANG, F., DOKSUM, K. & TSUI, K.-W. (2014). Principal component analysis (PCA) for high-dimensional data. PCA is dead. long live PCA. *Perspectives on Big Data Analysis: Methodologies and Applications* **622**, 1–22.

ZOU, H., HASTIE, T. & TIBSHIRANI, R. (2006). Sparse principal component analysis. *J. Comp. Graph. Stat.* **15**, 265–286.

A Exploring the distribution of the noise

The key point for visualization when $m > 2$ is how the distributions of the entities ε_{ij} and ε_{ik} depend on n and $\sigma_1^2, \dots, \sigma_n^2$, and whether they can be considered as noise compared to the scaling and approximate rotation matrix. We explore these questions by simulations and theoretical results, specifically in the case of normally distributed data. The distributions of the eigenvalues and eigenvectors are first evaluated theoretically for large sample size, n , using asymptotic theory and secondly through simulations of standard normally distributed scores $z_{ij} \sim \mathcal{N}(0, 1)$.

A.1 Large sample results

If the standardized population scores are standard normally distributed, $z_{ij} \sim \mathcal{N}(0, 1)$, and $\sigma_1^2 > \dots > \sigma_m^2$, then \mathbf{W} is Wishart distributed

$$\mathbf{W} \sim W_m(\text{diag}(\sigma_1^2, \dots, \sigma_m^2), n - 1),$$

where the matrix $\text{diag}(\sigma_1^2, \dots, \sigma_m^2)$ have the eigenvalues σ_j^2 and $\mathbf{e}_j = [0, \dots, 1, \dots, 0]^T$, the j th unit vector with a single 1 at position j , as the corresponding eigenvectors. Muirhead (2009, Corollary 9.4.1) gives the properties and distributions of the sample eigenvalues and eigenvectors of a Wishart matrix:

Firstly, when $n \rightarrow \infty$, all sample eigenvalues $\mathbf{v}_j(\mathbf{W})$ will be asymptotically independent of each other and of the sample eigenvectors $d_j(\mathbf{W})$. Secondly, the sample eigenvectors will converge to a normal distribution

$$n^{1/2}(\mathbf{v}_j(\mathbf{W}) - \mathbf{e}_j) \xrightarrow{d} \mathcal{N}(0, \Sigma_v)$$

and the covariance matrix

$$\Sigma_v = \sum_{i=1, i \neq j}^m \frac{\sigma_i^2 \sigma_j^2}{(\sigma_j^2 - \sigma_i^2)} \mathbf{e}_i \mathbf{e}_i^T = \text{diag} \left(\frac{\sigma_j^2 \sigma_1^2}{(\sigma_j^2 - \sigma_1^2)^2}, \dots, 0, \dots, \frac{\sigma_j^2 \sigma_m^2}{(\sigma_j^2 - \sigma_m^2)^2} \right).$$

We can insert the unit vectors or eigenvectors of \mathbf{W} directly in the results of Muirhead (2009). Further, the sample eigenvalues will also converge in distribution to

$$n^{1/2}(d_j(\mathbf{W}/n) - \sigma_j^2) \xrightarrow{d} \mathcal{N}(0, 2\sigma_j^4).$$

These results establish the asymptotic distribution of the sample eigenvalues and eigenvectors for large sample size, n , and by fixing the population scores to 1, $z_{ij} = 1$, for all i, j , the asymptotic distribution of ε_{ij} and ε_{ik} is given by the multivariate Delta method. The ε_{ij} is a function of the independent j th eigenvalue $d_j(\mathbf{W}/n)$ (where we move the scaling of n to the matrix \mathbf{W} for simplicity) and the entries of the j th eigenvector $\mathbf{v}_j(\mathbf{W})$:

$$\varepsilon_{ij} = f(d_j(\mathbf{W}/n), v_{j1}(\mathbf{W}), \dots, v_{jm}(\mathbf{W})) = \sqrt{\frac{1}{d_j(\mathbf{W}/n)}} \sum_{l \neq j, k}^m \sigma_l v_{jl}(\mathbf{W}).$$

Now, ε_{ij} will converge in distribution as

$$n^{1/2} (f(d_j(\mathbf{W}/n), v_{j1}(\mathbf{W}), \dots, v_{jm}(\mathbf{W})) - f(\sigma_j^2, 0, \dots, 0)) \rightarrow N(0, \tau_{11}),$$

where

$$\tau_{11} = \left(\frac{\partial f}{\partial d_j(\mathbf{W}/n)} \right)^2 \text{var}(d_j(\mathbf{W})) + \sum_{l=1, l \neq j, k}^m \left(\frac{\partial f}{\partial v_{jl}(\mathbf{W})} \right)^2 \text{var}(v_{jl}(\mathbf{W})),$$

and the partial derivatives are given

$$\left. \frac{\partial f}{\partial d_j(\mathbf{W}/n)} \right|_{(\sigma_j^2, 0, \dots, 0)} = -\frac{1}{2} d_j(\mathbf{W}/n)^{-3/2} \sum_{j \neq l, k}^m \sigma_l v_{jl}(\mathbf{W}) \Big|_{(\sigma_j^2, 0, \dots, 0)} = 0,$$

and

$$\left. \frac{\partial f}{\partial v_{jl}(\mathbf{W})} \right|_{(\sigma_j^2, 0, \dots, 0)} = \sigma_j \sqrt{\frac{1}{d_j(\mathbf{W}/n)}} \Big|_{(\sigma_j^2, 0, \dots, 0)} = \frac{\sigma_l}{\sigma_j},$$

and we get

$$\tau_{11} = \sum_{l=1, l \neq j, k}^m \frac{\sigma_l^2}{\sigma_j^2} \text{var}(v_{jl}(\mathbf{W})) = \sum_{l=1, l \neq j, k}^m \frac{\sigma_l^4}{(\sigma_j^2 - \sigma_l^2)^2}.$$

Together, the distribution of ε_{ij} and ε_{ik} will converge, as all variables are independent, to

$$n^{1/2} \begin{bmatrix} \varepsilon_{ij} \\ \varepsilon_{ik} \end{bmatrix} \xrightarrow{d} \mathcal{N} \left(\mathbf{0}, \text{diag} \left[\sum_{l=1, l \neq j, k}^m \frac{\sigma_l^4}{(\sigma_j^2 - \sigma_l^2)^2}, \sum_{l=1, l \neq j, k}^m \frac{\sigma_l^4}{(\sigma_k^2 - \sigma_l^2)^2} \right] \right), \quad n \rightarrow \infty.$$

The variance of this expression can be, as stated in the main paper, rewritten in terms of the ratio of the signal strengths, such that the asymptotic variance expression will be the following:

$$\text{var}(\varepsilon_{ij}) = \frac{1}{n} \sum_{l=1, l \neq j, k}^m \left(\frac{\sigma_j^2}{\sigma_l^2} - 1 \right)^{-2} + O(n^{-1}).$$

This shows that the variance of the noise terms only depend to the ratio between the signal strengths and their absolute value. The consequence is that the noise can become large if one the components in the pair has one or more neighboring components with similar signal strength σ_l^2 .

A.2 Simulations

The small sample situation of ε_{ij} can be explored by simulations, and the distribution is quantified through the mean and standard deviation. Particularly, we investigate how the standard deviation depend on n and $\sigma_1^2, \dots, \sigma_m^2$. The set-up is the following: the number of spiked components is fixed, $m = 5$, and the important pair is the first and second component scores $j = 1, k = 2$ with the signal strengths

$$\sigma_1^2 = 12, \quad \sigma_2^2 = 8,$$

while σ_3^2 will vary between 0.2 and 1.4 and $\sigma_4^2 = 0.1$ and $\sigma_5^2 = 0.02$ will be kept fixed.

Figure 3 displays graphically the simulated values of the standard deviation of ε_{i1} and ε_{i2} . The figure illustrates how the standard deviation decreases as the sample size n increases from 40 to 240, closely following the asymptotic rate of $n^{-1/2}$. The standard deviation of ε_{i1} and ε_{i2} are shown by dashed and solid lines, respectively, for three different values of σ_3^2 in blue, red and green. The smallest difference between σ_1^2 and σ_2^2 and all the other signal strengths is of course given by σ_3^2 and both ratios will change for different values of σ_3^2 . When σ_3^2 is doubled from 0.7 to 1.4, the standard deviation of ε_{i1} and ε_{i2} also approximately doubles. The 4:3 ratio between σ_1^2 and σ_2^2 is also reflected in the standard deviation, as the ratio between the standard deviation of ε_{i1} and ε_{i2} is also approximately 4/3.

Figure 4 displays graphically the simulated values of the standard deviation of ε_{i1} and ε_{i2} for $j = 1$ and $k = 2$ as a function of σ_3^2 when the sample size is fixed, $n = 60$, and σ_2^2 is given three different values, shown in green, blue and red. The standard deviation of both ε_{i1} (dashed line) and ε_{i2} (solid line) will increase when the value of σ_3^2 increases, as the ratios σ_1^2/σ_3^2 and σ_2^2/σ_3^2 will also increases. But when σ_2^2 is larger in absolute value, then the ratio σ_2^2/σ_3^2 will increase more as σ_3^2 increases. We see this as the green solid curve in Figure 4 increases faster with σ_3^2 than the blue and red solid curve . We will have the

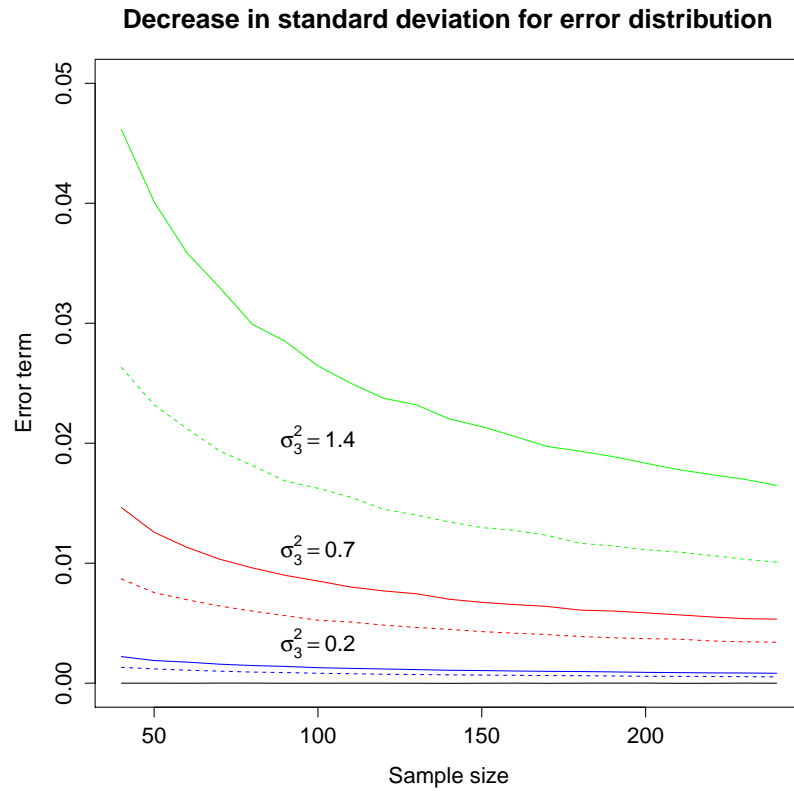


Figure 3: For $m = 5$, the standard deviation of the noise ε_{i1} (dashed curve) and ε_{i2} (solid curve), based on 10 000 simulations of normally distributed variables, for increasing sample size and decreasing difference between λ_2 and λ_3 (blue, red and green curve).

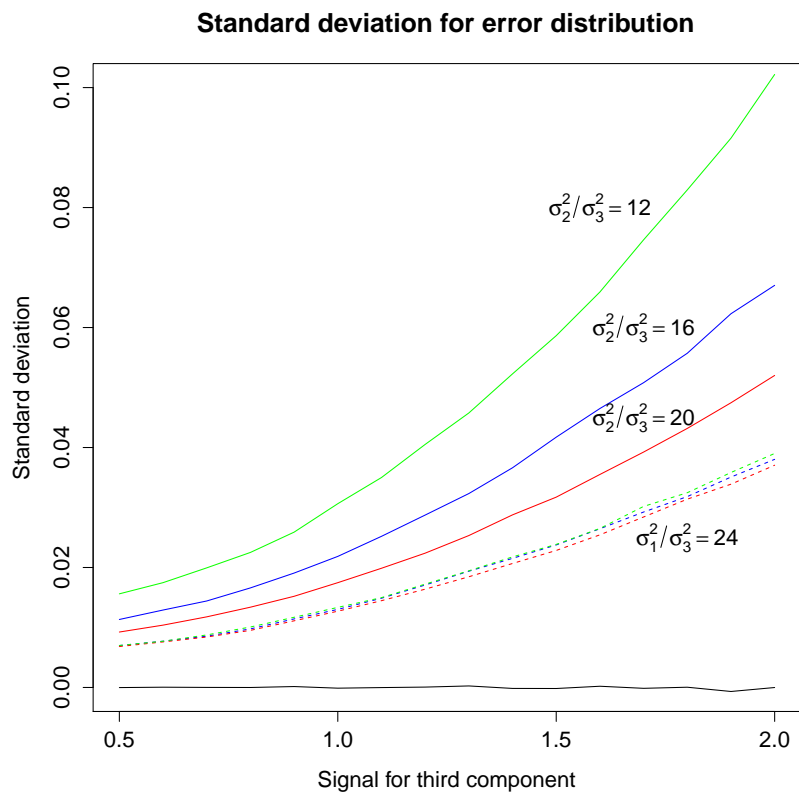


Figure 4: For $m = 5$ and fixed sample size $n = 60$, the standard deviation of ε_{i1} (dashed curve) and ε_{i2} (solid curve), based on 10 000 simulations of normally distributed variables. Blue, red and green curve display different ratio between signals of the second and third component.

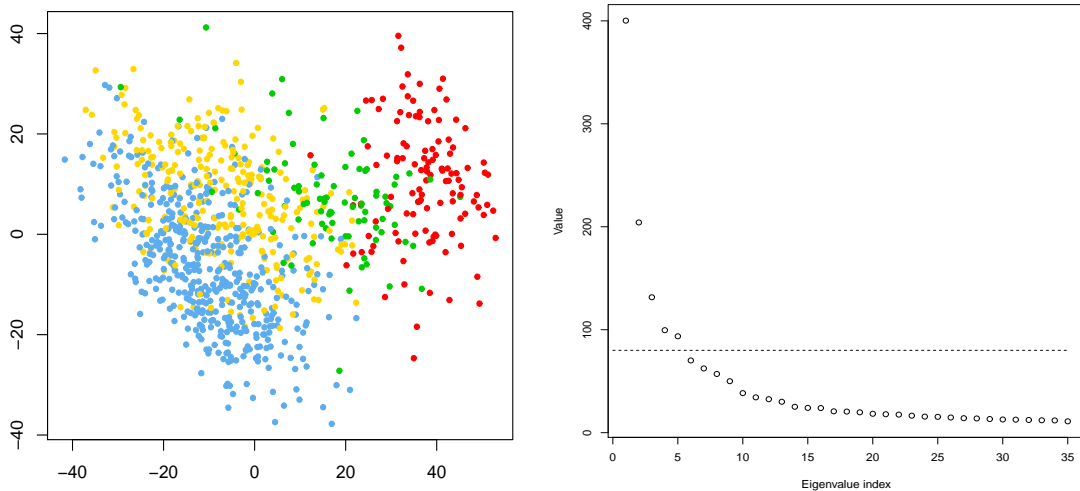


Figure 5: First and second component scores of gene expression data coloured according to breast cancer subtype. Scree plot of the 35 first eigenvalues.

opposite effect when σ_2^2 is set to a large value. In both cases, the standard deviation of ε_{i1} remains unchanged when σ_2^2 changes, as this will not affect the ratio σ_1^2/σ_3^2 .

When the population scores are standard normally distributed, their value will be of magnitude 1 and one can observe from Figure 3 and 4 that the standard deviation of ε_{ij} is of magnitude 10^{-2} for reasonable sample sizes and signal strengths. The second part in (6) in the main paper will therefore be negligible compared to the population scores and the first part of (6), and ε_{ij} can be considered as noise. However, how large the sample size needs to be for ε_{ij} to be negligible, depends specifically on the signal strengths $\sigma_1^2, \dots, \sigma_m^2$ and m , in particular the largest ratio between the relevant signal strengths and the rest.

B Example: Gene expression in cancer

To illustrate reasonable values for the parameters σ_j^2 and n , we use expression data from 3000 genes in the Metabric study (Perou et al., 2000). The first and second principal components scores from the data are shown in Figure 5, coloured according to breast cancer subtype. We use the Scree plot to attain five spiked eigenvalues, $m = 5$, as seen in Figure 5 and by dividing the eigenvalues by the number of variables, 3000, we get an

approximate estimate of the signal strengths:

$$\sigma_1^2 = 0.133, \quad \sigma_2^2 = 0.068, \quad \sigma_3^2 = 0.044, \quad \sigma_4^2 = 0.033, \quad \sigma_5^2 = 0.031.$$

Based on these estimates, Eq. (7) can be used to find how large sample size is needed to have a negligible noise terms: if the standard deviation of the noise term for $j = 1, k = 2$ should be less than 0.15, the sample size must be larger than 19 for the first component and larger than 217 for the second component due to the similar third component.